สมบัติทางโครงสร้างและทางแสงของฟิล์มบางดีบุกไดออกไซด์เจือเหล็กและพลวงเตรียมโดยวิธีสเปรย์ไพโรไลซิส

Structural and Optical Properties of Fe and Sb-doped Tin Dioxide Films prepared by the Spray Pyrolysis Method

จำเนียร พุฒพันธ์ และ สุวัฒน์ ผาบจันดา*
ภาควิชาเคมี และศูนย์ความเป็นเลิศด้านนวัตกรรมทางเคมี (ศนค.)
คณะวิทยาศาสตร์ มหาวิทยาลัยอุบลราชธานี
*E-mail: pabchanda@gmail.com

บทคัดย่อ

งานวิจัยนี้เป็นการเตรียมฟิล์มบางดีบุกไดออกไซด์เจือเหล็กและพลวงบนฐานรองกระจกโดยวิธีสเปรย์ไพโรไลซิส ใช้ $SnCl_4 \cdot 5H_2O$ เป็นสารตั้งต้น $FeCl_3$ และ $SbCl_3$ เป็นสารเจือ ตามลำดับ ศึกษาผลของระดับการเจือเหล็กและพลวง (6 และ 12 ร้อยละโดยโมล) ต่อสมบัติทางโครงสร้างและทางแสงของฟิล์มบางดีบุกไดออกไซด์โดยเทคนิค XRD และ UV-Vis ผล XRD แสดงความกว้างที่ครึ่งหนึ่งของความสูงพีคเพิ่มขึ้นตามการเพิ่มปริมาณเหล็กและพลวงในฟิล์ม ซึ่งเป็นสาเหตุขององศาความเป็นผลึกต่ำลงตามความเข้มข้นของสารเจือสูงขึ้น ฟิล์มบางเจือเหล็กและพลวงที่ระดับความเข้มข้น 0 ถึง 12 ร้อยละโดยโมล มีค่าการส่งผ่านแสงเฉลี่ยในช่วงวิสิเบิลและค่าแถบช่องว่างพลังงานลดลงตามการเพิ่มปริมาณสารเจือ ผลที่ได้แสดงให้เห็นว่าสมบัติของฟิล์มบางดีบุกไดออกไซด์เจือเหล็กและพลวงขึ้นอยู่กับระดับการเจือสารเจือ

คำสำคัญ : สเปรย์ไพโรไลซิส ดีบุกไดออกไซด์ ฟิล์มบาง

Abstract

In this research, Fe- and Sb-doped tin dioxide thin films on glass substrate were fabricated by the spray pyrolysis technique using $SnCl_4 \cdot 5H_2O$ as a precursor and $FeCl_3$ and $SbCl_3$ as dopants respectively. The effect of Fe- and Sb-doping levels (6 and 12 mol%) on the structural and optical properties of tin dioxide thin films were investigated by XRD and UV-Vis techniques. X-ray diffraction analysis showed that the full widths at half maxima (FWHM) of diffraction peaks were increased with increasing Fe and Sb content in the films, which was the reason for the lower degree of crystallinity corresponding to higher dopant concentrations. The average optical transparency (%T) in the visible region and optical band gap (E_g) of thin films for Fe and Sb doping levels in the range 0 to 12 mol% decreased with increasing doping concentrations. The results revealed that properties of Fe- and Sb-doped SnO_2 thin films depended on the doping levels.

Keywords: Spray pyrolysis; Tin dioxide; Thin film

Introduction

Transparent conducting oxide (TCO) has been extensively studied for its use in applications such as gas sensors [1], dye-sensitized solar cells [28], organic light emitting diodes [2], 2010), transparent electrodes for flat panel displays [3], and thermoelectric energy conversions [4]

Tin dioxide (SnO_2) is extensively used in a variety of TCO thin films because of a wide band gap n-type semiconductor (E_g = 3.5-4.0 eV) and low electrical resistance with high optical transparency in the visible region (400–800 nm) electromagnetic spectrum [5]. The coexistence of tin interstitials and oxygen vacancies in SnO_2 gives it a unique combination of transport and optical properties [4]. The SnO_2 as the host is mostly preferred because of its interesting optical and electrical properties and widespread applicability. Doping the SnO_2 nanostructures with metals and metal oxides without altering optical transparency is the primary means of controlling electrical conductivity [6] and this plays an increasingly important role in technological applications of these materials. The 3d transition metal ions as dopants with open d-shell electronic configurations have various unique properties including optical properties or other physical properties of their host semiconductors [7]**.** In fact, doping SnO_2 nanostructures with transition metals such as Fe or Sb affects the structural properties, increases the conductivity values, and keeps the optical transparency in the visible region. The chemical and physical properties are modified by metal or metal oxide additives. By Fe- and Sb-doping, oxygen vacancies are produced in one-dimensional SnO_2. The oxygen vacancy has a great influence on the physical and chemical properties and also strongly attracts the Fe and Sb ions. As a consequence, transition metal–oxygen vacancies–transition metal groups are common in SnO_2 doped with Fe or Sb. In order to meet the demand of the potential application offered by metal oxides, it is pivotal to control the doping with extrinsic elements to tune their structural and optical properties of SnO_2 films [8].

Fe- and Sb-doped SnO_2 thin films can be prepared by various techniques such as chemical vapor deposition [9], r. f. sputtering [2], sol-gel spin coating [10], sol-gel dip coating [11] and spray pyrolysis [12],[1]. Among the various deposition techniques available, spray pyrolysis is the most convenient method because of its simple and inexpensive experimental arrangement, ease of adding doping materials, high growth rate, and mass production capability for uniform large area coatings, which are desirable for industrial applications [13].

In this study, SnO_2, SnO_2:Fe and SnO_2:Sb thin films deposited on micro-slide glass substrate were prepared by the spray pyrolysis technique. Structural and optical properties of thin films were characterized by X-ray diffraction (XRD) and UV-Vis spectroscopy analysis methods, respectively.

Experiment

Thin films of SnO_2, SnO_2:Fe and SnO_2:Sb were prepared by the homemade spray pyrolysis experimental setup. The schematic diagrams of the experimental set-up and other details have been reported elsewhere [14]. The precursor solution was prepared by dissolving a 8.75 g (0.025 mol) of $SnCl_4 \cdot 5H_2O$ in 104.0 ml of mixed solvent (a mixture of 90.0 ml ethanol, 10.0 ml of double distilled water and 4.0 ml of HCl) [15]. The solution was stirred for about 2 h at 60 °C and kept at room temperature for 24 h before spraying. The amount of $FeCl_3$ and $SbCl_3$ was varied by 6 and 12 mol% for Fe- and Sb-doping levels. The solution flow rate (3.0 ml/min^{-1}) was controlled by filtered compressed air at a carried air pressure of 0.2 kg/cm^{-2}. The normalized distance between the spray nozzle and the substrate was

about 60 cm. Optical micro-slide glass plates with an effective area of 7.5 x 2.5 cm were used as substrates. The substrates were cleaned with cleaning solution as (1:3 volume by volume) HNO_3: HCl, rinsed with ethanol in ultrasonic bath and heated at 500 $^{\circ}$C for 1 hour before spraying. The spray liquid, prepared from the solution with different concentrations of $FeCl_3$ and $SbCl_3$ were sprayed onto the hot substrates where pyrolysis and film deposition occurred. The normalized deposition temperature was $500\pm10^{\circ}$C for SnO_2, Fe- and Sb-doped SnO_2 films. The spray time was maintained at 5 min and the waiting time allowed between successive spraying applications was 10 min. The x-ray diffraction patterns of pure and doped SnO_2 films were recorded by Philips X'pert MPD using Cu K_α radiation (wavelength 0.154059 nm) radiation with 2θ in the range 20° to 60°. The average crystallite sizes corresponding to the (110) plane of the film was calculated using the Scherrer's formula [4]. In addition, the lattice distance (*d*), lattice parameters (*a*-axis, *c*-axis) and cell volume (*V*) of thin films could also be calculated [16],[17].

The optical absorption and transparency studies were performed in the wavelength range of 300-1,100 nm using Lambda 25 UV-Vis double beam spectrophotometer. The thickness of film (t) was determined by using the optical transmission spectra (%T) and the following equation: $t = \lambda_1\lambda_2/2\eta(\lambda_1-\lambda_2)$ where λ_1 and λ_2 are the two consecutive peaks in transmission spectra and η is the refractive index of SnO_2 (η = 1.95). The direct optical band gaps (E_g) for various Fe- and Sb-doping levels were obtained by optical absorption measurements and plotting $(\alpha h\nu)^2$ versus photon energy ($h\nu$) and using the following relation: $(\alpha h\nu)^2 = A(h\nu-E_g)$ where α, A and E_g is the absorption coefficient, constant and the direct band gap of the material, respectively [4],[18].

Results and discussion

Fig. 1 shows the X-ray diffraction patterns of SnO_2 SnO_2:Fe and SnO_2:Sb thin films for different doping levels (6 and 12 mol%). The XRD patterns of all films with different dopants and various doping levels were polycrystalline SnO_2 films with rutile structure having all peaks corresponding to the specific planes as shown in Fig. 1 [1]. No peaks corresponding to iron oxide and antimony oxide films were observed. Previous works [19],[17],[20],[21]. reported that the positions of the XRD peaks corresponding to different h k l values were seen to be shifted towards lower angles when doping with Fe or Sb. In the present work, the 2θ values of (110) plane of tin oxide doped with Fe-doping at 6 and 12 mol% were 26.75° and 26.74°, whereas Sb-doping levels were 26.73° and 26.70°, respectively. The results showed that the main peak position of (110) plane for SnO_2 films were slightly shifted to lower 2θ values with increasing Fe- or Sb-doping concentrations compared with SnO_2 (26.79°). The results indicated that Sn atoms were replaced by Fe or Sb atoms in SnO_2 lattice [21],[15]. Moreover, Sb-doping changed the preferred orientation of SnO_2 thin films [22],[15]. For Sb-doped SnO_2 thin films (Fig. 1d and 1e), the preferred orientation changed from 110 to 200 plane with 6 mol% Sb-doping concentration, while the relative diffraction intensity of 200 plane decreased with 12 mol% Sb-doping. This observation indicated that Sn atom was also replaced by Sb atom in the lattice sites of SnO_2 structure.

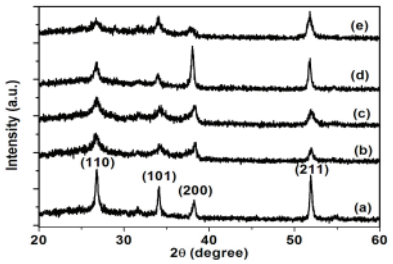

Fig. 1 X-ray diffraction patterns of SnO_2 thin films for different dopants and various doping levels: (a) SnO_2, (b) SnO_2:Fe (6 mol%), (c) SnO_2:Fe (12 mol%), (d) SnO_2:Sb (6 mol%) and (e) SnO_2:Sb (12 mol%).

Table 1 shows the full width at half maxima (FWHM) of SnO_2 thin films for different dopants and various doping levels. The FWHM values of tin oxide doped with Fe-doping at 6 and 12 mol% were 0.784° and 0.864°, whereas Sb-doping levels were 0.518° and 0.757°, respectively. The results showed that the FWHM of films increased with increasing Fe- or Sb-doping level compared with pure SnO_2 (0.394°). This also suggested that Fe or Sb atoms were incorporated into the SnO_2 lattice, results in the decrease of crystallinity of films [15],[23],[10],[4]. The crystallite size of SnO_2, SnO_2:Fe and SnO_2:Sb thin films corresponding to the peak of (110) plane were calculated using Scherrer's formula. The crystallite size of tin oxide doped with Fe-doping at 6 and 12 mol% were 10.287 and 9.342 nm, whereas Sb-doping levels were 15.588 and 10.662 nm, respectively. The crystallite sizes slightly decreased with increasing doping concentrations compared with pure SnO_2 (20.465 nm). This indicated that the increase of Sb or Fe atoms introduction in SnO_2 matrix should have slightly reduced crystallite growth which is related to decrease of crystallite size [23]. Moreover, the FWHM values of Fe-doping were higher than those of Sb-doping at the same concentrations. Fe-doping influence on the crystallite growth in SnO_2 film was more than Sb-doping [10],[24],[25],[26].

Table 1 Summary of the XRD parameters at (110) plane of SnO_2 thin films for different dopants and various doping levels

Thin film	2-theta (degree)	FWHM (degree)	crystallite size (nm)	a (Å)	c (Å)	Lattice distance, d (Å)	Cell volume (Å^3)
SnO_2	26.79	0.394	20.465	4.701	3.169	3.324	70.040
SnO_2:Fe (6 mol%)	26.75	0.784	10.287	4.707	3.159	3.328	69.982
SnO_2:Fe (12 mol%)	26.74	0.864	9.342	4.709	3.150	3.330	69.834
SnO_2:Sb (6 mol%)	26.73	0.518	15.588	4.711	3.183	3.331	70.661
SnO_2:Sb (12 mol%)	26.70	0.757	10.662	4.716	3.182	3.335	70.778

Doping influence on the lattice distance (*d*), lattice parameters ((*a*′ and *'c'*) and cell volume values (*V*) of SnO_2 thin films are illustrated in Table 1. It was found that the lattice distance of (110) plane increased with increasing Fe- or Sb-doping levels compared with SnO_2 films. This change in the lattice distance ($d_{1\ 1\ 0}$) was attributed to the strain of the crystal lattice caused by the difference in ionic radius between host and dopant [21],[10],[4]. The lattice parameters and cell volume of Sb-doped SnO_2 films were larger than pure tin oxide. In the process of Sb-doping, Sb^{3+} (ionic radius 0.90 Å) would be converted

to Sb^{5+} (ionic radius 0.62 Å) during a heating. A high amount of Sb-doping was attributed to the reduction of a part of Sb^{5+} to Sb^{3+}, which resulted in the high ratio of Sb^{3+}/Sb^{5+} and hence an increase in cell volume of SnO_2 [16]. However, for Fe-doping, 'c' parameter and cell volume of tin oxide decreased with increased Fe content. The observations indicated that Fe ions were incorporated into SnO_2 lattice in the form of Fe^{3+} (ionic radius 0.64 Å) with not present of Fe^{2+} (ionic radius 0.77 Å) [10]. Moreover, the lattice distance, lattice parameters and cell volume of Fe- doped SnO_2 were lower than Sb-doping at the same doping levels. These results can be explained by the fact that the ionic radius of Fe^{3+} (ionic radius 0.64 Å) is smaller than Sb^{3+} (ionic radius 0.90 Å). Doping smaller ions of Fe^{3+} were incorporated into the lattice of Sn^{4+} (ionic radius 0.72 Å) that was given a lower cell volume of Fe-doping compared with Sb-doping in SnO_2 films [25], [26].

Fig. 2 shows the optical transmittance of films in the range 300–1100 nm. As shown, the values of average transmittance of the films decreased with increasing Fe- or Sb-doping level, which was related to the reduction of crystalline size and escalation of light scattering [4],[22]. Highly Sb-doped SnO_2 films elaborated by spray pyrolysis presented a bluish coloration due to a charge transfer between the two oxidation states of antimony, Sb^{3+} and Sb^{5+} [27].

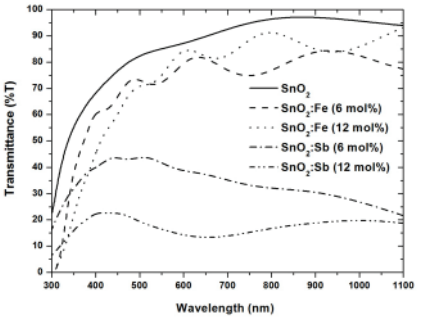

Fig. 2 Optical transparency of SnO_2 thin films for different dopants and various doping levels

It has been shown that Fe- or Sb-doping has an influence on optical band gap (E_g))of the SnO_2 films [2],[4],[11]. As seen in Table 2, optical band gap of tin oxide doped with Fe-doping levels at 6 and 12 mol% were 3.72 eV and 3.62 eV, while for Sb-doping levels they were 3.65 and 3.54 eV, respectively. The optical band gaps decreased with increasing doping concentrations compared with pure SnO_2 (3.79 eV). Increasing doping levels reduced the optical band gap, which resulted in an incorporation of Fe or Sb ions into the SnO_2 crystal structures to promote electron and hole concentration. That led to the charge-transfer transition between the d-electrons of metal dopant ions and the SnO_2 conduction or valence band [11]. The other reason for optical band gap reduction might have been due to the appearance of the Fe-Sn or Sb-Sn metallic compounds, as can be seen in XRD analysis results [4]. Furthermore, the optical band gap of Sb-doped SnO_2 was lower than Fe-doping at the same doping levels [21],[23].

Table 2 Transparency (%T), film thickness, and the direct optical band gap of SnO_2 thin films for different dopants and various doping levels.

Thin film	Transparency (%T)	Film thickness (nm)	Direct optical band gap (eV)
SnO_2	85.75	618	3.79
SnO_2:Fe (6 mol%)	83.84	582	3.72
SnO_2:Fe (12 mol%)	76.51	678	3.62
SnO_2:Sb (6 mol%)	38.84	538	3.65
SnO_2:Sb (12 mol%)	15.97	882	3.54

Conclusion

This work reported the preparation and characterization of Fe- and Sb-doped tin oxide thin films at various doping levels. These films were deposited by the spray pyrolysis technique. The XRD studies of the samples showed a polycrystalline structure with clear characteristic peak of the rutile phases SnO_2 crystallites with tetragonal structure. Increasing doping levels reduced the crystalinity and crystallite growth of SnO_2 films. The transparency and optical band gap (E_g) of thin films for Fe- and Sb-doping levels in the range 0 to 12 mol% decreased with increased doping levels.

Acknowledgements

Financial support from the Center of Excellence for Innovation in Chemistry (PERCH-CIC), Office of the Higher Education Commission, Ministry of Education is gratefully acknowledged. Also, the authors are grateful to the Faculty of Science, Ubon Ratchathani University for the use of all equipment.

References

[1] Elangovan, E. and Ramamurthi, K. 2005. **A study on low cost-high conducting fluorine and antimony-doped tin oxide thin films.** Applied Surface Science, 249: 183–196.

[2] Montero, J.; Herrero, J. and Guillen, C. 2010. **Preparation of reactively sputtered Sb-doped SnO_2 thin films: Structural, electrical and optical properties.** Solar Energy Materials & Solar Cells, 94: 612–616.

[3] Budak, S.; Miao, G. X.; Ozdemir, M.; Chetry, K. B. and Gupta, A. 2006. **Growth and characterization of single crystalline tin oxide (SnO_2) nanowires.** Journal of Crystal Growth, 291: 405-411.

[4] Mohagheghi, M. M. B.; Shahtahmasebi, N. and Alinejad, M. R. 2009. **Fe-doped SnO_2 transparent semi-conducting thin films deposited by spray pyrolysis technique: Thermoelectric and p-type conductivity properties.** Solid State Sciences, 11: 233–239.

[5] Amanullah, F. M.; Pratap, K. J. and Babu, V. H. 1998. **Compositional analysis and depth profile studies on undoped and doped tin oxide films prepared by spray technique.** Materials Science and Engineering, 52: 93–98

[6] Amanullah, F. M.; Mobarak, M. S.; Al-Dhariam, A. M. and Shibani, K. M. 1999. **Development of spray technique for the preparation of thin films and characterization of tin oxide transparent conductors.** Materials Chemistry and Physics, 59: 247–253.

[7] Jain, G. and Kumar, R. 2004. **Electrical and optical properties of tin oxide and antimony doped tin oxide films.** Optical Materials, 26: 27–31.

[8] Matsushima, Y.; Nemoto, Y.; Yamazaki, T.; Maeda, K. and Suzuki, T. 2003. **Fabrication of SnO_2 particle-layer on the glass substrate using electrospray pyrolysis method and the gas sensitivity for H_2.** Sensors and Actuators, 96: 133–138.

[9] Assia, S.; Ratiba, O.; Mahdi, M. E. and Mohamed, K. 2009. **Optical Reflectance of Pure and Doped Tin Oxide: From Thin Films to Poly-Crystalline Silicon/Thin Film Device.** International Journal of Chemical and Biological Engineering, 21: 48-51.

[10] Rani, S.; Roy, S. C.; Karar N. and Bhatnagar, M. C. 2007. **Structure, microstructure and photoluminescence properties of Fe doped SnO_2 thin films.** Solid State Communications, 141: 214–218.

[11] Soitah, T. N.; Yang, C. and Sun, L. 2010. **Structural, optical and electrical properties of Fe-doped SnO_2 fabricated by sol–gel dip coating technique.** Materials Science in Semiconductor Processing, 13: 125–131.

[12] Korotcenkov, G.; Brinzari, V. and Boris, I. 2008. **(Cu, Fe, Co, or Ni)-doped tin dioxide films deposited by spray pyrolysis: doping influence on film morphology.** Journal of Material Science, 43**:** 2761–2770.

[13] Ma, H. L.; Hao, X. T.; Ma, J.; Yang, Y. J.; Huang, J.; Zhang, D. H. and Xu, X. G. 2002. **Thickness Dependence of Properties of SnO_2:Sb Films Deposited on Flexible Substrates.** Applied surface science, 191**:** 313-318.

[14] Patil, P. S.; Kawara, R. K.; Seth, T.; Amalnerkar, D. P. and Chigare, P. S. 2003. **Effect of substrate temperature on structural, electrical and optical properties of sprayed tin oxide (SnO_2) thin films.** Ceramics International, 29: 725–734.

[15] Shanthi, S.; Subramanian, C. and Ramasamy, P. 1999. **Growth and characterization of antimony doped tin oxide thin films.** Journal of Crystal Growth, 197: 858–864.

[16] Ming, J.; Zu, Y. T.; Ying, G. Y.; Juan, D. Z. and Ling, L. J. 2005. **Preparation of antimony doped nanoparticles by hydrothermal method.** The Transactions of Nonferrous Metals Society of China, 15: 702-705.

[17] Mishra, A. K.; Sinha, T. P.; and Yopadhyay, S. B. and Das, D. 2011. **Structural and magnetic properties of nanocrystalline Fe-doped SnO_2.** Materials Chemistry and Physics, 125**:** 252–256.

[18] Xiao, X.; Dong, G.; Shao, J.; He, H. and Fan, Z. 2010. **Optical and electrical properties of SnO_2: Sb thin films deposited by oblique angle deposition.** Applied Surface Science, 256: 1636–1640.

[19] Nomura, K.; Barrero, C.; Sakuma, J. and Takeda, M. 2006. **Mossbauer study of SnO_2 powders doped with dilute ^{57}Fe prepared by a sol-gel method.** Journal of Physics, 56**:** 75-81.

[20] Chakraborty, S.; Sen, A. and Maiti, H. S. 2006. **Selective detection of methane and butane by temperature modulation in iron doped tin oxide sensors.** Sensors and Actuators, 115: 610–613.

[21] Shokr, E. Kh.; Wakkad, M. M.; Ghanny, H. A. A. and Ali, H. M. 2000. **Sb-doping effects on optical and electrical parameters of SnO_2 films.** Journal of Physics and Chemistry of Solids, 61: 75–85.

[22] Hammad, T. M. and Hejazy, N. K. 2011. **Structural, Electrical and Optical Properties of ATO Thin Films Fabricated by Dip Coating Method.** International Nano Letters, 1: 123–128.

[23] Vaishampayan, M. V.; Deshmukh, R. G.; Walke, P. and Mulla, I. S. 2008. **Fe-doped SnO_2 nanomaterial: A low temperature hydrogen sulfide gas sensor.** Materials Chemistry and Physics, 109**:** 230–234.

[24] Jung, D. W. and Park, D. W. 2009. **Synthesis of nano-sized antimony-doped tin oxide (ATO) particles using a DC arc plasma jet.** Applied Surface Science, 255: 5409–5413.

[25] Kong, J.; Deng, H.; Yang, P. and Chu, J. 2009. **Synthesis and properties of pure and antimony-doped tin dioxide thin films fabricated by sol–gel technique on silicon wafer.** Materials Chemistry and Physics, 114: 854–859.

[26] Krishnakumar, T.; Jayaprakash, R.; Pinna, N.; Phani, A. R.; Passacantando, M. and Santucci, S. 2009. **Structural, optical and electrical characterization of antimony-substituted tin oxide nanoparticles.** Journal of Physics and Chemistry of Solids, 70: 993–999.

[27] Elangovan, E.; Singha, M. P.; Dharmaprakash, M. S. and Ramamurthi, K. 2004. **Some Physical Properties of Spray Deposited SnO_2 Thin Films**. Journal of Optoelectronics and Advanced Materials, 6: 197–203.

[28] Thangaraju, B. 2002. **Structural and electrical studies on highly conducting spray deposited fluorine and antimony doped SnO_2 thin films from $SnCl_2$ precursor.** Thin Solid Films, 402: 71–78.